BioOne COMPLETE

Kolotl, n. gen. (Scorpiones: Diplocentridae), a New Scorpion Genus from Mexico

Authors: Santibáñez-López, Carlos E., Francke, Oscar F., and Prendini, Lorenzo

Source: American Museum Novitates, 2014(3815) : 1-14

Published By: American Museum of Natural History

URL: https://doi.org/10.1206/3815.1

BioOne Complete (complete.BioOne.org) is a full-text database of 200 subscribed and open-access titles in the biological, ecological, and environmental sciences published by nonprofit societies, associations, museums, institutions, and presses.

Your use of this PDF, the BioOne Complete website, and all posted and associated content indicates your acceptance of BioOne's Terms of Use, available at www.bioone.org/terms-of-use.

Usage of BioOne Complete content is strictly limited to personal, educational, and non - commercial use. Commercial inquiries or rights and permissions requests should be directed to the individual publisher as copyright holder.

BioOne sees sustainable scholarly publishing as an inherently collaborative enterprise connecting authors, nonprofit publishers, academic institutions, research libraries, and research funders in the common goal of maximizing access to critical research.

Downloaded From: https://bioone.org/journals/American-Museum-Novitates on 04 Jun 2024
Terms of Use: https://bioone.org/terms-of-use

AMERICAN MUSEUM NOVITATES

Number 3815, 28 pp. October 16, 2014

Kolotl, n. gen. (Scorpiones: Diplocentridae), a New Scorpion Genus from Mexico

CARLOS E. SANTIBÁÑEZ-LÓPEZ,[1,2] OSCAR F. FRANCKE,[2] AND LORENZO PRENDINI[3]

ABSTRACT

The monophyly and phylogenetic position of *Diplocentrus* Peters, 1861, has remained ambiguous since the first published phylogenetic analysis of diplocentrid relationships, in which it was rendered paraphyletic by the placement of exemplar species from two other diplocentrid genera, *Bioculus* Stahnke, 1968, and *Didymocentrus* Kraepelin, 1905. The discovery of two diplocentrids with neobothriotaxic pedipalps, *Diplocentrus magnus* Beutelspacher and López-Forment, 1991, and *Diplocentrus poncei* Francke and Quijano-Ravell, 2009, from the central Mexican states of Guerrero and Michoacán, respectively, raised further questions about the limits of *Diplocentrus*. A recent phylogenetic analysis of 29 species of *Diplocentrus* and five exemplar species of the most closely related genera, based on 95 morphological characters and 4202 aligned nucleotides from DNA sequences of five markers in the nuclear and mitochondrial genomes, recovered the monophyly of *Diplocentrus*, excepting two neobothriotaxic species from central Mexico, justifying their removal from *Diplocentrus*. In the present contribution, *Kolotl*, n. gen. is created to accommodate the two species, *Kolotl magnus* (Beutelspacher and López-Forment, 1991), n. comb., and *Kolotl poncei* (Francke and Quijano-Ravell, 2009), n. comb., and both are redescribed.

[1] Posgrado en Ciencias Biológicas, Universidad Nacional Autónoma de México, Distrito Federal, México.
[2] Colección Nacional de Arácnidos, Instituto de Biología, Distrito Federal, México.
[3] Scorpion Systematics Research Group, Division of Invertebrate Zoology, American Museum of Natural History.

Copyright © American Museum of Natural History 2014 ISSN 0003-0082

Downloaded From: https://bioone.org/journals/American-Museum-Novitates on 04 Jun 2024
Terms of Use: https://bioone.org/terms-of-use

INTRODUCTION

The scorpion family Diplocentridae Karsch, 1880, comprises nine genera and approximately 120 species, distributed mostly in the New World, except for *Nebo* Simon, 1878 (9 species), and two species of *Heteronebo* Pocock, 1899, which occur in the Middle East (Prendini, 2000; Sissom and Fet, 2000). The most diverse genus of the family, *Diplocentrus* Peters, 1861, currently comprises approximately 58 species (Santibáñez-López et al., 2013a). *Diplocentrus* is endemic to North and Central America, ranging from the southwestern United States (Arizona, New Mexico, and Texas) to northern Honduras (Sissom and Fet, 2000), but its greatest diversity (47 described species) and endemism occurs in mainland Mexico. Although most species of *Diplocentrus* are fossorial, these scorpions exhibit considerable morphological variation, from small species such as *Diplocentrus bereai* Armas and Martín-Frías, 2004, with total adult length of 20–30 mm, to rather large species such as *Diplocentrus taibeli* (Caporiacco, 1938), with total adult length of 80–90 mm.

The monophyly, taxonomic and geographical limits of *Diplocentrus*, long a source of confusion, remained ambiguous since the first published phylogenetic analysis of diplocentrid relationships, based on exemplar species included in a larger analysis of scorpionoid phylogeny (Prendini, 2000). *Diplocentrus* was paraphyletic in most of Prendini's (2000) analyses, due to the placement of exemplar species from two other diplocentrid genera, *Bioculus* Stahnke, 1968, and *Didymocentrus* Kraepelin, 1905, the validity of which had been disputed by several authors (Williams and Lee, 1975; Francke, 1978; Sissom, 1990; Stockwell, 1992). Prendini (2000) suggested that one or both genera should be synonymized with *Diplocentrus*, or the generic limits of *Diplocentrus* redefined, to restore its monophyly.

Diplocentrus poncei Francke and Quijano-Ravell, 2009, the first species of *Diplocentrus* with accessory trichobothria on the pedipalp chela and patella, was subsequently described. Francke and Quijano-Ravell (2009) also discovered accessory trichobothria on the pedipalp patella of *Diplocentrus magnus* Beutelspacher and López-Forment, 1991. These two species from the central Mexican states of Michoacán and Guerrero, respectively, are unique among diplocentrids in possessing neobothriotaxic pedipalps, raising questions about their phylogenetic placement within *Diplocentrus*.

Recently, Santibáñez-López et al. (in press) presented a phylogenetic analysis of 29 species of *Diplocentrus* and five exemplar species of the three diplocentrid genera most closely related to it (*Bioculus*, *Didymocentrus* and *Tarsoporosus* Francke, 1978). The analysis was based on 95 morphological characters and 4202 aligned nucleotides from DNA sequences of five markers in the nuclear and mitochondrial genomes. The resulting phylogeny recovered the monophyly of *Diplocentrus* with the exception of the two neobothriotaxic species from central Mexico, justifying their removal from *Diplocentrus*. In the present contribution, *Kolotl*, n. gen., is created to accommodate the two species, *Kolotl magnus* (Beutelspacher and López-Forment, 1991), n. comb., and *Kolotl poncei* (Francke and Quijano-Ravell, 2009), n. comb., and both are redescribed.

METHODS

Material examined is deposited in the following collections: American Museum of Natural History, New York (AMNH), with tissue samples stored in the Ambrose Monell Cryocollection

Downloaded From: https://bioone.org/journals/American-Museum-Novitates on 04 Jun 2024
Terms of Use: https://bioone.org/terms-of-use

(AMCC); Colección Aracnológica de la Facultad de Biología, Universidad Michoacana de San Nicolás de Hidalgo, Morelia, Michoacán, Mexico (CAFBUM); Colección Nacional de Arácnidos, Instituto de Biología, Universidad Nacional Autónoma de México, Mexico City (CNAN).

Scorpion higher classification follows Prendini and Wheeler (2005). Nomenclature and mensuration follows Stahnke (1970), except for trichobothria (Vachon, 1974), carination of the metasoma (Francke, 1977) and pedipalps (Prendini, 2000), pedipalp chela finger dentition (Soleglad and Sissom, 2001) and carapacial surfaces (Prendini et al., 2003). Spiniform macrosetae on the leg basitarsi, informative in the systematics of family Scorpionidae Latreille, 1802 (Prendini et al., 2003), have also proven informative at the generic level in Diplocentridae (Santibáñez-López et al., 2013a, 2013b), and are employed here.

Observations were made using Nikon SMZ-800 and SMZ-1500 stereomicroscopes. Measurements, given in millimeters, were obtained with an ocular micrometer calibrated at 10×. Digital images were taken under visible and UV light with a Microptics ML-1000 digital imaging system, equipped with a Nikon DS80 camera, or a Nikon SMZ-800 with Nikon Coolpix S10 VR camera attachment. The focal planes of images were fused using CombineZM software (Hadley, 2008) and composite images edited with Adobe Photoshop CS6.

Distribution maps were generated in ArcView Ver. 3.2 (ESRI), using georeferenced locality records, a base map from ArcView and a digital elevation model from the CGIAR Consortium for Spatial Information (Jarvis et al., 2008). Locality records without geographical coordinates were retroactively georeferenced using Google Earth.

SYSTEMATICS

Family Diplocentridae Karsch, 1880
Subfamily Diplocentrinae Karsch, 1880

Key to Identification of the Species of *Kolotl*, n. gen.

– Pedipalp patella, retrolateral surface with 15 trichobothria (2 *est*, 3 *em*), ventral surface with four trichobothria; chela, ventral surface with four trichobothria; legs, coloration pale, contrasting with dark coloration of tergites and metasoma ……. *Kolotl magnus*, n. comb.

– Pedipalp patella, retrolateral surface with 20–23 trichobothria, ventral surface with 8–14 trichobothria; chela, ventral surface with 9–13 trichobothria; legs, tergites and metasoma coloration dark, similar ……. *Kolotl poncei*, n. comb.

***Kolotl*,** n. gen.

Figures 1–14; tables 1–3

Diplocentrus (part): Beutelspacher and López-Forment, 1991: 34–40; Beutelspacher, 2000: 30; Francke and Quijano-Ravell, 2009: 659–663; Volschenk and Prendini, 2008: 236; Sissom and Reddell, 2009: 21; Contreras-Félix and Santibáñez-López, 2011: 62, 63.

Type Species: *Diplocentrus poncei* Francke and Quijano-Ravell, 2009 [= *Kolotl poncei* (Francke and Quijano-Ravell, 2009), n. comb.].

Downloaded From: https://bioone.org/journals/American-Museum-Novitates on 04 Jun 2024
Terms of Use: https://bioone.org/terms-of-use

Etymology: The generic name is derived from the Nahuatl word for scorpion, *kolotl*. It is masculine in gender.

Diagnosis: *Kolotl* is most closely related to *Didymocentrus* (fig. 1), with which it shares the presence of punctation on the nongranular surfaces of the carapace and pedipalps, disproportionate development of the retrolateral secondary carina of the pedipalp chela, relative to the digital carina, and a similar pattern of spiniform macrosetae on the basitarsi of legs III and IV. Species of *Kolotl* differ from *Didymocentrus* in the absence of a distinct concavity on the prolateral surface of the pedipalp chela in adult males, basal to trichobothria *ib* and *it*. *Kolotl* may be further separated from *Didymocentrus* and all other diplocentrids by the following characters. *Kolotl* is unique among diplocentrids in possessing neobothriotaxic pedipalps, with accessory trichobothria on the retrolateral and ventral surfaces of the patella in both species of the genus and on the ventral surfaces of the chela in *K. poncei*. The cheliceral dentition is also unique in *Kolotl*: the dorsal distal denticle of the cheliceral movable finger is equal to the ventral distal denticle and the subdistal denticle equal to the median denticle whereas in other diplocentrids the ventral distal denticle is larger than the dorsal distal denticle and the subdistal denticle smaller than the median denticle. The pedipalp chela finger dentition of *Kolotl* is also unique: the prolateral, median and retrolateral denticle rows are well defined from the proximal quarter to the tip of the finger, and continuous, i.e., not interrupted by larger denticles. Also unlike other diplocentrids, the anteromedian longitudinal sulcus of the carapace is complete in *Kolotl*.

Included Taxa: Two species: *Kolotl magnus*, n. comb.; *Kolotl poncei*, n. comb.

Distribution: *Kolotl* is endemic to western Mexico, and recorded from eight localities in the states of Guerrero and Michoacan.

Kolotl magnus (Beutelspacher and López-Forment, 1991), n. comb.

Figures 1–2, 4, 6A, 7A, 8A, 9, 11, 14A–D; tables 1–3

Diplocentrus magnus Beutelspacher and López-Forment, 1991: 33–40; Fritts and Sissom, 1996: 44; Kovařík, 1998: 130; Sissom and Fet, 2000: 340; Teruel, 2003: 50, 55; Francke and Quijano-Ravell, 2009: 662, 663, Volschenk and Prendini, 2008: 236; Sissom and Reddell, 2009: 21.

Type Material: **MEXICO**: GUERRERO: *Municipio de Acapulco de Juárez*: holotype ♀ (CNAN-T0122), Puerto Marquéz, 2 km W [16°48.984′N 99°50.779′W], 8.vii.1974, W.J. Mautz, collected at entrance of a crevice in a granite boulder. Paratype ♂ (CNAN-T0123), Puerto Marquéz, 5 km W [16°49.401′N 99°51.594′W], 21.vi.1985, W. López-Forment.

FIGURE 1. Most parsimonious tree (length, 4682; CI, 0.322; RI, 0.471, fit, 525.43; adjusted homoplasy, 381.57) obtained by simultaneous cladistic analysis of 95 morphological characters and 4202 aligned nucleotides from five markers in the nuclear and mitochondrial genomes for 35 species in six diplocentrid scorpion genera, with implied weighting under $k = 3$ (Santibáñez-López et al., in press). Unambiguous morphological synapomorphies optimized on branches: black squares indicate uniquely derived apomorphic states, white squares indicate parallel derivations of apomorphic states; numbers above squares indicate characters, numbers below indicate states. See appendix 1 for character list.

Downloaded From: https://bioone.org/journals/American-Museum-Novitates on 04 Jun 2024
Terms of Use: https://bioone.org/terms-of-use

Downloaded From: https://bioone.org/journals/American-Museum-Novitates on 04 Jun 2024
Terms of Use: https://bioone.org/terms-of-use

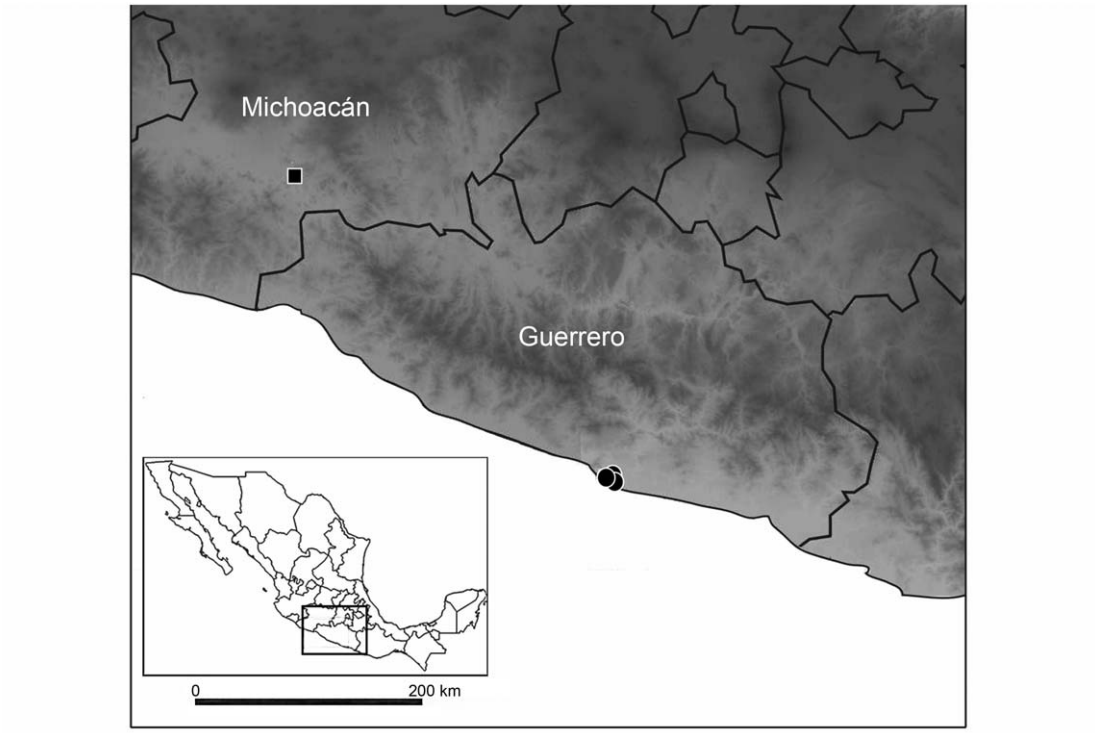

FIGURE 2. Map of central Mexico, plotting known locality records for the two species of *Kolotl*, n. gen.: *Kolotl magnus* (Beutelspacher and López-Forment, 1991), n. comb., black circles, and *Kolotl poncei* (Francke and Quijano-Ravell, 2009), n. comb., black square.

Additional Material: **MEXICO**: GUERRERO: *Municipio de Acapulco de Juárez:* Cumbres de Llano Largo, 16°49.505′N 99°49.999′W, 371 m, 19.vi.2006, O.F. Francke, H. Montaño, and A. Ballesteros, 3 juv. (CNAN), 1 juv. (AMCC [LP 7029]); Puerto Marquéz [16°47.689′N 99°49.239′W], W. López-Forment, 1 juv. (CNAN-S00712); Puerto Marquéz, 2 km W [16°48.984′N 99°50.780′W], 28.v.1974, 1 ♀ (CNAN-S00710), 10.vii.1974, W. López-Forment, 1 ♀ (CNAN-S00713); Puerto Marquéz, 4 km N [16°49.717′N 99°49.255′W], 5.vii.1975, W. López-Forment, 2 juv. (CNAN-S00714); Puerto Marquéz, 5 km W [16°49.401′N 99°51.594′W], 21.vi.1985, W. López-Forment, 1 ♀ (CNAN-S00711).

Diagnosis: This species can be separated from the other species in the genus as follows: *Kolotl magnus* possesses fewer trichobothria on the retrolateral and ventral surfaces of the pedipalp patella (15 and 4 trichobothria, respectively) than *K. poncei* (20–23 and 8–14, respectively). The pedipalp chela is orthobothriotaxic, with four trichobothria on the ventral surface in *K. magnus* ($n = 4$) but neobothriotaxic, with 9–13 trichobothria on the ventral surface in *K. poncei*. The coloration of the legs is pale and contrasts with the dark coloration of the tergites and metasoma in *K. magnus*, whereas the coloration of the legs, tergites and metasoma is dark and similar in *K. poncei*. The counts of spiniform macrosetae on the telotarsi of legs I and II are higher in *K. magnus* (4/6:5/7) than in *K. poncei* (3/5:4/6).

Redescription: Based on holotype ♀ and paratype ♂. Selected measurements in table 1.

Downloaded From: https://bioone.org/journals/American-Museum-Novitates on 04 Jun 2024
Terms of Use: https://bioone.org/terms-of-use

FIGURE 3. Habitat at type locality of *Kolotl poncei* (Francke and Quijano-Ravell, 2009), n. comb.: El Vado, Municipio de La Huacana, Michoacan, Mexico. **A.** Crevices in rock outcrop. **B.** Rock wall.

Downloaded From: https://bioone.org/journals/American-Museum-Novitates on 04 Jun 2024
Terms of Use: https://bioone.org/terms-of-use

Table 1. Selected measurements (mm) for type specimens of *Kolotl magnus* (Beutelspacher and López-Forment, 1991), n. comb., and *Kolotl poncei* (Francke and Quijano-Ravell, 2009), n. comb., in the Colección Nacional de Arácnidos (CNAN), Instituto de Biología, Universidad Nacional Autónoma de México, Mexico City.

		K. magnus		*K. poncei*	
	Type	Paratype	Holotype	Holotype	Paratype
	Sex	juv. ♂	♀	♂	♀
	CNAN	T0123	T0122	T0392	T0393
Carapace	length	7.6	13.5	11.0	13.2
	anterior width	5.5	9.7	7.5	10.0
	posterior width	7.9	14	12.3	14.7
Chela	length	13.1	26	23.9	26.2
	width	3.4	6.0	4.9	5.5
	height	5.7	10.5	8.8	10
	movable finger	7.9	15	12.8	13.2
	fixed finger	5.9	9.8	9.0	10.2
Patella	length	6.8	12	11.8	12
	width	2.8	4.8	3.8	4.5
Femur	length	6.1	11	11.5	11.5
	width	2.5	4.0	4.0	4.7
Mesosoma	length	22.4	39.4	31.7	37.1
Metasoma I	length	3.9	6.1	5.2	4.9
	width	3.5	5.5	4.9	5.5
	height	2.6	4.0	3.6	4.4
Metasoma II	length	4.1	6.6	5.5	5.6
	width	3.0	4.8	4.0	4.8
	height	2.5	4.0	3.5	4.2
Metasoma III	length	4.2	7.2	5.9	5.9
	width	2.9	4.7	3.7	4.5
	height	2.5	4.0	3.5	3.9
Metasoma IV	length	4.7	8.0	6.5	6.7
	width	2.9	4.4	3.5	4.5
	height	2.4	3.8	3.3	3.7
Metasoma V	length	6.1	10.2	8.6	8.9
	width	2.6	4.0	3.0	3.8
	height	2.1	3.3	3.0	3.5
Metasoma	total length	23	38.1	31.7	32.0
Telson	total length	6.0	6.9	8.2	9.9
	vesicle length	4.6	4.7	7.1	8.0
	vesicle width	2.9	5.0	3.4	4.5
	vesicle height	2.2	4.1	3.0	3.6
	aculeus length	1.4	2.2	1.1	1.9
Hemispermatophore	total length	–	–	10.0	–
	lamella length	–	–	7.1	–
	capsule width	–	–	0.9	–
Total length		59	97.9	82.6	92.2

Downloaded From: https://bioone.org/journals/American-Museum-Novitates on 04 Jun 2024
Terms of Use: https://bioone.org/terms-of-use

Table 2. Pectinal tooth count (number of teeth per pecten) in *Kolotl magnus* (Beutelspacher and López-Forment, 1991), n. comb., and *Kolotl poncei* (Francke and Quijano-Ravell, 2009), n. comb., summarized as number of male and female pectines observed with corresponding tooth count, including data from Francke and Quijano-Ravell (2009).

	K. magnus		*K. poncei*	
Total counts	♂	♀	♂	♀
12		1		
13		3		1
14	1	5		8
15	3			7
16			4	4
17			13	2
18			11	
19			3	

Total length: Adult, 70–97 mm.

Coloration: Base color, dark brown. Cheliceral manus, dorsal surface yellowish with reticulate infuscation. Carapace, anterior margin dark brown, posterior margin light brown to orange. Coxosternum pale brown to pale yellow. Pedipalps dark brown to slightly reddish, with darker carinae. Legs pale yellow, contrasting with dark mesosomal tergites, uniformly and faintly infuscate. Mesosoma dark brown (♂) or brownish orange (♀); tergites weakly (♂) to moderately (♀) infuscate; sternites pale yellow to orange. Metasoma and telson dark brown.

Carapace: Anterior margin weakly setose; anteromedian notch moderate, U-shaped, slightly granular. Anteromedian longitudinal sulcus narrow, shallow; anteromedian longitudinal suture present. Nongranular surfaces of frontal lobes and interocular surface moderately punctate; surfaces around median ocular tubercle smooth to punctate. One pair of median ocelli, situated anteromedially; three pairs of subequal lateral ocelli (fig. 7A).

Chelicerae: Movable finger, ventral distal denticle equal to dorsal distal denticle; subdistal denticle equal to median denticle (fig. 6A).

Pedipalps: Pedipalps neobothriotaxic, type C. Patella, retrolateral surface with 15 trichobothria (3 *et*, 2 *est*, 3 *em*, 2 *esb*, 5 *eb*) (fig. 9A); ventral surface with four trichobothria (fig. 9B). Chela, ventral surface with four trichobothria (fig. 11C); trichobothrium *ib* aligned with *it*, both trichobothria situated proximal to base of fixed finger (fig. 11D).

Femur width greater than height; dorsal intercarinal surface flat, sparsely granular; retrolateral intercarinal surface smooth (fig. 9A); ventral intercarinal surface flat, punctate; prolateral intercarinal surface coarsely and sparsely granular; dorsal prolateral carina well developed, comprising large spiniform granules; dorsal retrolateral carina weakly to moderately developed, comprising few large granules; ventral retrolateral carina obsolete; ventral prolateral carina moderately developed, comprising large spiniform granules.

Patella dorsal, retrolateral and ventral intercarinal surfaces punctate; prolateral intercarinal surface finely and sparsely granular; proximal tubercle moderately developed, comprising two large granules; dorsal prolateral carina obsolete; dorsal median carina weakly to moderately

Downloaded From: https://bioone.org/journals/American-Museum-Novitates on 04 Jun 2024
Terms of Use: https://bioone.org/terms-of-use

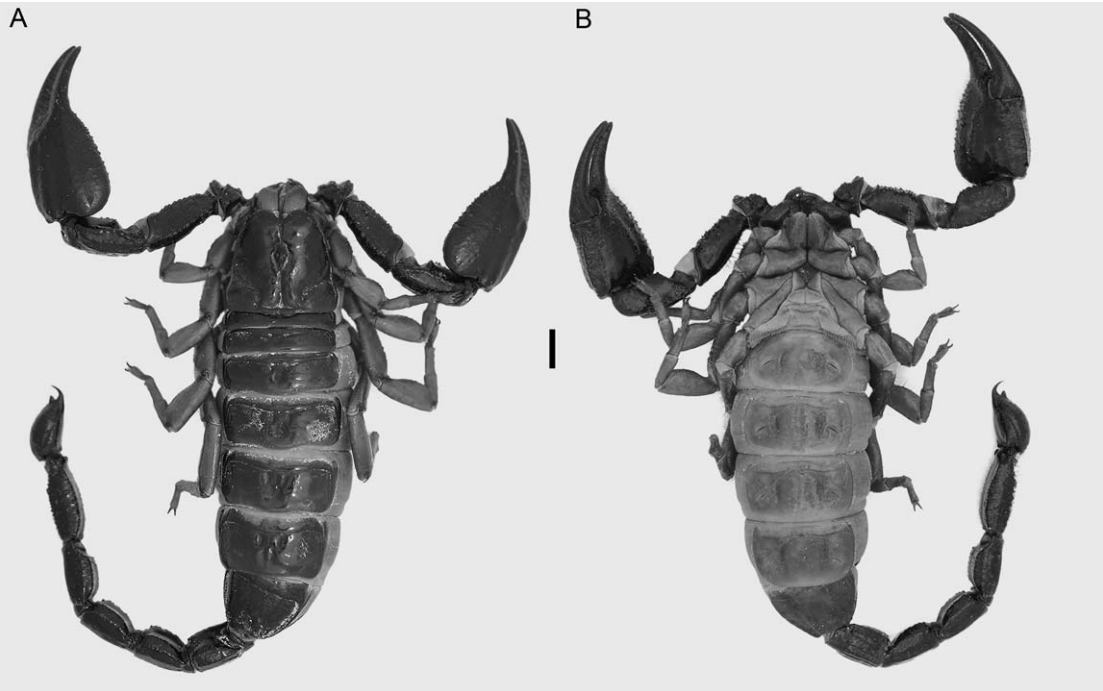

FIGURE 4. *Kolotl magnus* (Beutelspacher and López-Forment, 1991), n. comb., holotype ♀ (CNAN), habitus, dorsal aspect (**A**) and ventral aspect (**B**). Scale bar = 5 mm.

developed, smooth; dorsal retrolateral, retrolateral median, and ventral retrolateral carinae weakly developed to obsolete, smooth; ventral median carina obsolete; ventral prolateral carina moderately developed, granular.

Chela manus rounded, height greater than width (♀, subadult ♂); sparsely setose; dorsal intercarinal surface finely and sparsely granular to slightly reticulate; prolateral and retrolateral intercarinal surfaces punctate; dorsal median carina weakly developed, granular; dorsal secondary carina weakly to moderately developed, smooth (♀); digital and ventral retrolateral carinae weakly developed to obsolete, smooth; retrolateral secondary carina weakly to moderately developed, smooth (♀); dorsal secondary and retrolateral secondary carinae equally developed, more developed than digital carina; ventral median carina moderately developed, distal edge disconnected from retrolateral movable finger condyle and directed toward a point between prolateral and retrolateral movable finger condyles, less than half the distance between trichobothria Et_1 and V_1; ventral prolateral and prolateral ventral carinae obsolete; prolateral median and prolateral dorsal carinae weakly developed, granular. Chela fixed finger moderately curved; length less than femur length and patella length; dorsal surface punctate and moderately setose proximally; prolateral surface shallowly concave; retrolateral surface flat; prolateral carina weakly developed (fig. 11A). Chela movable finger, prolateral, median and retrolateral denticle rows well defined from proximal quarter to tip of finger, and continuous, i.e., not interrupted by larger denticles (fig. 11B).

Legs: Legs I–IV, femora and tibiae, prolateral surfaces shagreened. Basitarsi, spiniform macrosetae (fig. 14A–D), I: prolateral subdistal, retrolateral distal, retrolateral subdistal; II: prolat-

Downloaded From: https://bioone.org/journals/American-Museum-Novitates on 04 Jun 2024
Terms of Use: https://bioone.org/terms-of-use

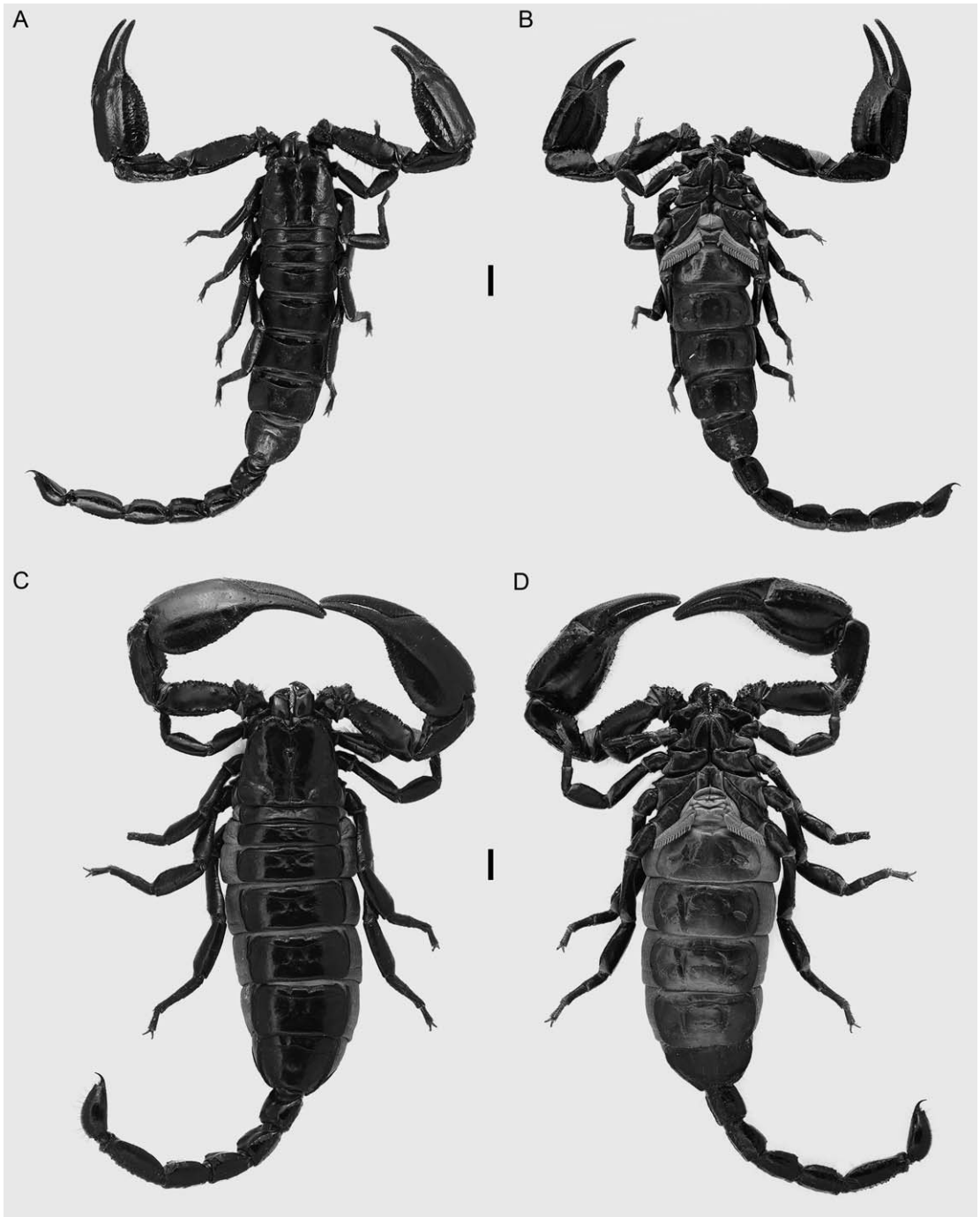

FIGURE 5. *Kolotl poncei* (Francke and Quijano-Ravell, 2009), n. comb., habitus, dorsal aspect (**A, C**) and ventral aspect (**B, D**). **A, B.** Paratype ♂ (AMNH). **C, D.** Paratype ♀ (CNAN). Scale bars = 5 mm.

Downloaded From: https://bioone.org/journals/American-Museum-Novitates on 04 Jun 2024
Terms of Use: https://bioone.org/terms-of-use

Table 3. Telotarsal spiniform macrosetal count (number of macrosetae in pro- and retroventral rows of telotarsi on legs I–IV) in *Kolotl magnus* (Beutelspacher and López-Forment, 1991), n. comb., and *Kolotl poncei* (Francke and Quijano-Ravell, 2009), n. comb., given as number of legs observed with corresponding pro- (p) and retroventral (r) setal count, including data from Francke and Quijano-Ravell (2009).

		K. magnus		*K. poncei*	
Leg	Count	p	r	p	r
I	2			1	
	3			50	
	4	14		1	1
	5		1		53
	6		13		
II	4	6		52	
	5	8		2	
	6		3		49
	7		11		5
III	4			1	
	5	11		52	
	6	2		1	2
	7		11		51
	8		2		
IV	5	10		53	
	6	4			
	7		6		51
	8		8		2

eral distal, prolateral subdistal, retrolateral distal, retrolateral subdistal, retrolateral medial; III and IV: prolateral distal, ventral distal, ventral subdistal, retrolateral distal. Telotarsi, counts of spiniform macrosetae in pro- and retroventral rows, 4/6:5/7:5/7:5/7–8 (table 3).

Pectines: Tooth count: 14–15, mode = 15 (♂); 12–15, mode = 14 (♀) (table 2).

Mesosoma: Tergites I–VI, pre- and posttergites smooth; VII, posterior margin finely granular. Sternites III–VII, smooth; VII, ventral submedian and ventral lateral carinae obsolete anteriorly, more strongly developed and smooth posteriorly.

Metasoma: Metasomal segments I–V, cross section terete; intercarinal surfaces punctate. Segments I–IV, dorsal lateral carinae obsolete to weakly developed, granular on I, weakly developed, granular on II, weakly to moderately developed, granular on III and IV; lateral supramedian carinae moderately developed, granular to crenulate on I and II, weakly developed, granular on III and IV; lateral inframedian carinae weakly developed, smooth on I and II, weakly developed to obsolete on III and IV; ventral lateral carinae moderately developed, smooth to crenulate on I and II; weakly developed to obsolete, smooth on III and IV; ventral submedian carinae moderately developed, smooth on I and II; weakly developed to obsolete, smooth on III and IV. Segment V, dorsal lateral carinae moderately developed, granular to serrate; lateral inframedian carinae

Downloaded From: https://bioone.org/journals/American-Museum-Novitates on 04 Jun 2024
Terms of Use: https://bioone.org/terms-of-use

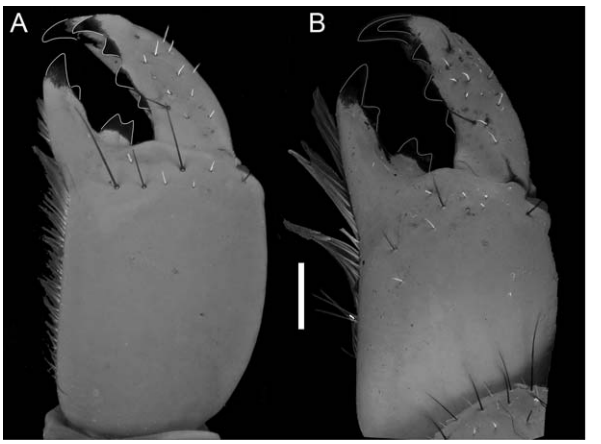

FIGURE 6. *Kolotl*, n. gen., dextral chelicerae, dorsal aspect, illustrating dentition. **A.** *Kolotl magnus* (Beutelspacher and López-Forment, 1991), n. comb., holotype ♀ (CNAN). **B.** *Kolotl poncei* (Francke and Quijano-Ravell, 2009), n. comb., paratype ♂ (AMNH). Scale bar = 1 mm.

moderately developed, granular; ventral median carina strongly developed, comprising subspiniform granules; ventral transverse carina well developed, incomplete, comprising six large, subspiniform granules; anal arch semicircular, anal subterminal carina well developed, comprising 10 subspiniform granules, anal terminal carina moderately developed, granular.

Telson: Telson, width/length ratio, 0.48 (♂), 0.72 (♀). Vesicle, dorsal surface smooth; lateral surfaces finely and sparsely granular; ventral surfaces coarsely granular anteriorly, finely and sparsely granular elsewhere. Subaculear tubercle stout, subconical.

Hemispermatophore: Unknown.

Distribution: *Kolotl magnus* is known from seven localities in close proximity, in the Municipio de Acapulco de Juárez on the south coast of Guerrero, Mexico (fig. 2).

Ecology: The known localities are situated in an area of tropical deciduous forest. Beutelspacher and López-Forment (1991) suggested that the species is troglobitic because it was collected inside a cave, but also noted that it inhabits cracks and crevices in rocks. Based on the criteria outlined by Volschenk and Prendini (2008), this species does not exhibit troglomorphies (e.g., absence or reduction of ocelli, absence of pigmentation, attenuation of legs and pedipalps) and its presence in a cave was probably accidental. The habitat and habitus are consistent with the semilithophilous ecomorphotype (Prendini, 2001).

Kolotl poncei (Francke and Quijano-Ravell, 2009), n. comb.

Figures 1–3, 5, 6B, 7B, C, 8B, C, 10, 12-13, 14E–H; tables 1–3

Diplocentrus poncei Francke and Quijano-Ravell, 2009: 659–663; Contreras-Félix and Santibáñez-López, 2011: 62, 63.

Type Material: **MEXICO**: MICHOACAN: *Municipio de La Huacana*: holotype ♂, 1 ♂, 3 ♀ (one with 24 offspring), 4 juv. ♂, 4 juv. ♀ paratypes (CNAN-T0392), El Vado, 17 km from

Downloaded From: https://bioone.org/journals/American-Museum-Novitates on 04 Jun 2024
Terms of Use: https://bioone.org/terms-of-use

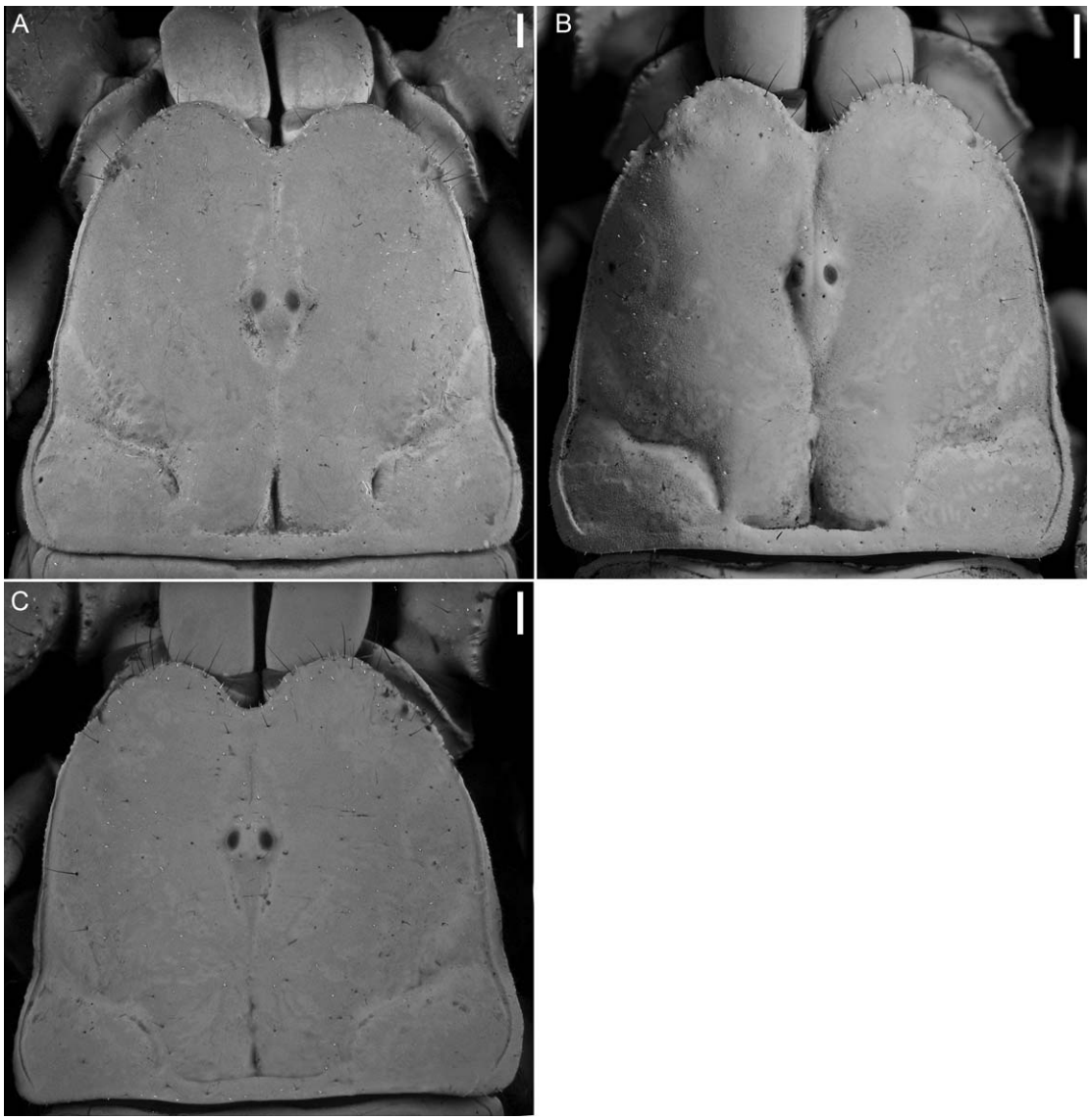

FIGURE 7. *Kolotl,* n. gen. carapace, dorsal aspect. **A.** *Kolotl magnus* (Beutelspacher and López-Forment, 1991), n. comb., holotype ♀ (CNAN). **B.** *Kolotl poncei* (Francke and Quijano-Ravell, 2009), n. comb., paratype ♂ (AMNH). **C.** *K. poncei*, paratype ♀ (CNAN). Scale bars = 1 mm.

Zicuiran to Churumuco, 18°48.908′N 101°54.976′W, 20.v.2007, O. Francke, J. Ponce, A. Quijano, M. Villaseñor and A. Ballesteros.

Additional Material: **MEXICO**: MICHOACAN: *Municipio de La Huacana*: El Vado, 17 km from Zicuiran to Churumuco, 18°48.908′N 101°54.976′W, 20.v.2007, O.F. Francke, J. Ponce, A. Quijano, M. Villaseñor, and A. Ballesteros, 1 juv. (AMCC [LP 7030]), 1.xi.2007, J. Ponce, A. Quijano and M. Villaseñor, 1 ♂ (CAFBUM), 30.vi.2008, O.F. Francke, J. Ponce, A. Quijano, and H. Montaño, 1 ♂, 7 juv. ♂, 3 juv. ♀ (CNAN), 1 ♂, 1 ♀ (AMNH).

Downloaded From: https://bioone.org/journals/American-Museum-Novitates on 04 Jun 2024
Terms of Use: https://bioone.org/terms-of-use

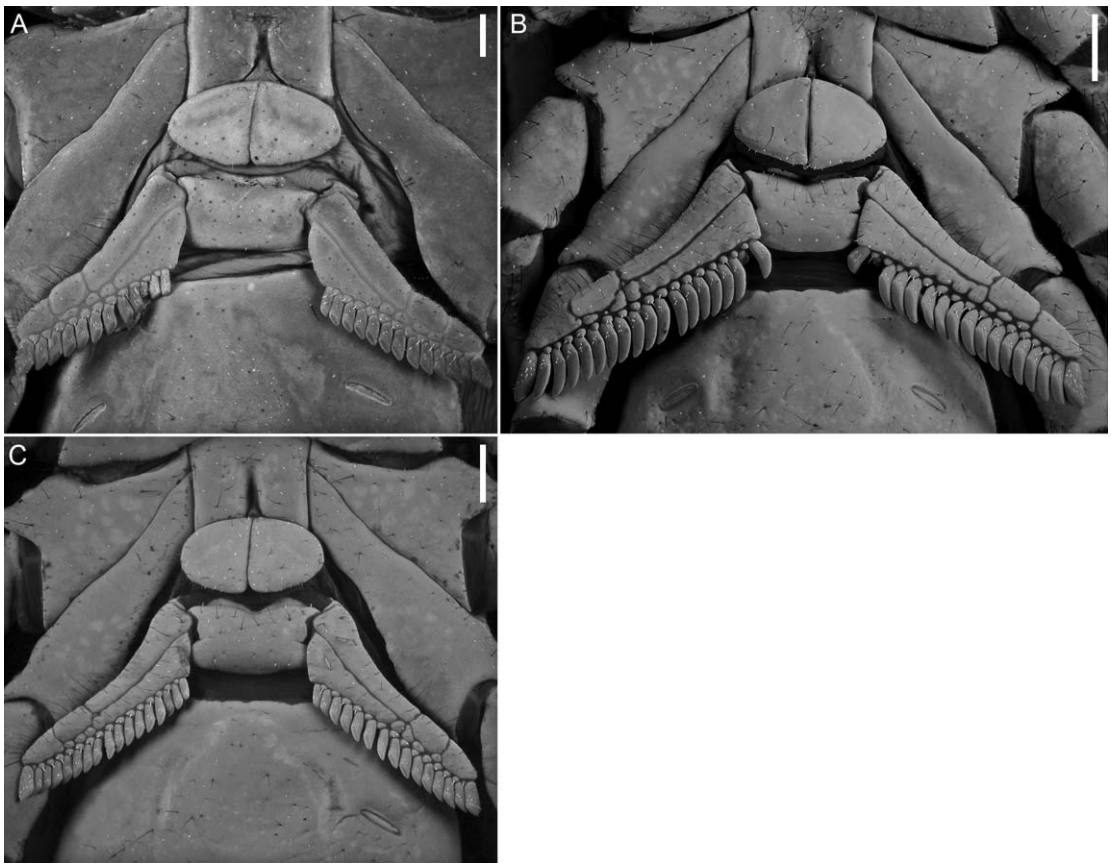

FIGURE 8. *Kolotl*, n. gen., sternum, genital operculum and pectines, ventral aspect. **A.** *Kolotl magnus* (Beutelspacher and López-Forment, 1991), n. comb., holotype ♀ (CNAN). **B.** *Kolotl poncei* (Francke and Quijano-Ravell, 2009), n. comb., paratype ♂ (AMNH). **C.** *K. poncei*, paratype ♀ (CNAN). Scale bars = 1 mm.

Diagnosis: This species can be separated from the other species in the genus as follows: *Kolotl poncei* possesses more trichobothria on the retrolateral and ventral surfaces of the pedipalp patella (20–23 and 8–14, respectively) than *K. magnus* (15 and 4 trichobothria, respectively). The pedipalp chela is neobothriotaxic, with 9–13 trichobothria on the ventral surface in *K. poncei* but orthobothriotaxic, with four trichobothria on the ventral surface in *K. magnus* (n = 4). The coloration of the legs, tergites and metasoma is dark and similar in *K. poncei*, whereas the coloration of the legs is pale and contrasts with the dark coloration of the tergites and metasoma in *K. magnus*. The counts of spiniform macrosetae on the telotarsi of legs I and II are lower in *K. poncei* (3/5:4/6) than in *K. magnus* (4/6:5/7).

Redescription: Based on holotype ♂ and paratype ♀. Selected measurements in table 1.

Total length: Adult, 70–97 mm.

Coloration: Base color, dark brown. Cheliceral manus, dorsal surface brownish orange with reticulate infuscation. Carapace, anterior margin dark brown, posterior margin brown to orange. Coxosternum brown to pale orange. Pedipalps dark brown with darker carinae. Legs dark brown, similar to dark mesosomal tergites, uniformly and faintly infuscate, tarsi light

Downloaded From: https://bioone.org/journals/American-Museum-Novitates on 04 Jun 2024
Terms of Use: https://bioone.org/terms-of-use

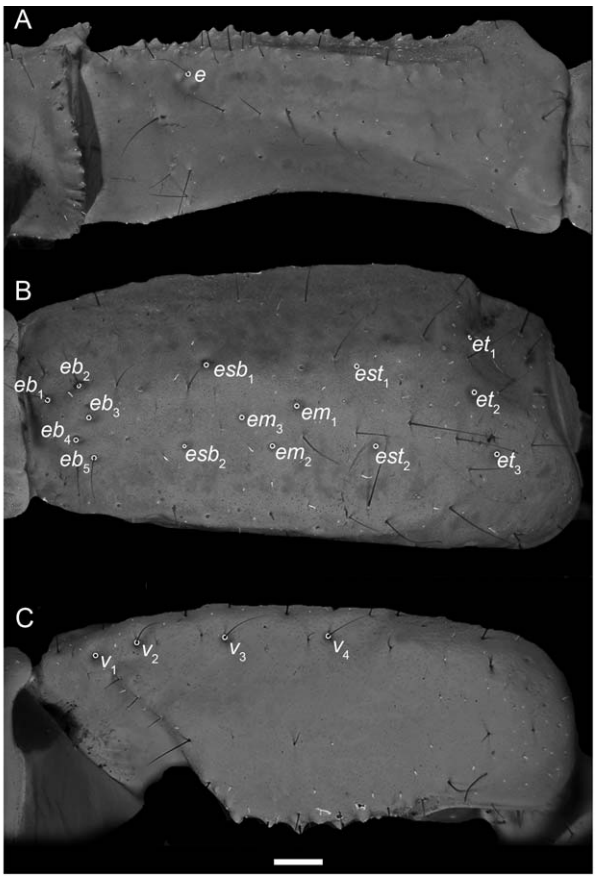

FIGURE 9. *Kolotl magnus* (Beutelspacher and López-Forment, 1991), n. comb., holotype ♀ (CNAN), dextral pedipalp femur, retrolateral aspect (**A**) and patella, retrolateral aspect (**B**) and ventral aspect (**C**), illustrating carinae and trichobothria. Scale bar = 1 mm. Abbreviations: ***e,*** external; ***eb,*** external basal; ***em,*** external medial; ***esb,*** external subbasal; ***est,*** external subterminal; ***et,*** external terminal; ***V,*** ventral.

brown to orange. Mesosoma dark brown; tergites weakly (♂) to moderately (♀) infuscate; sternites pale orange to brown. Metasoma dark brown. Telson pale to dark brown.

Carapace: Anterior margin moderately setose; anteromedian notch moderate, U-shaped, slightly granular. Anteromedian longitudinal sulcus narrow, shallow; anteromedian longitudinal suture present. Nongranular surfaces of frontal lobes and interocular surface moderately punctate; surfaces around median ocular tubercle smooth to punctate. One pair of median ocelli, situated anteromedially; three pairs of subequal lateral ocelli (fig. 7B, C).

Chelicerae: Movable finger, ventral distal denticle equal to dorsal distal denticle; subdistal denticle equal to median denticle (fig. 6B).

Pedipalps: Pedipalps neobothriotaxic, type C. Patella, retrolateral surface with 20–23 trichobothria (fig. 10B); ventral surface with 8–14 trichobothria (fig. 10C). Chela, ventral surface with 9–13 trichobothria (fig. 12C, 13B); trichobothrium *ib* aligned with *it*, both trichobothria situated proximal to base of fixed finger (fig. 12D, 13C).

Downloaded From: https://bioone.org/journals/American-Museum-Novitates on 04 Jun 2024
Terms of Use: https://bioone.org/terms-of-use

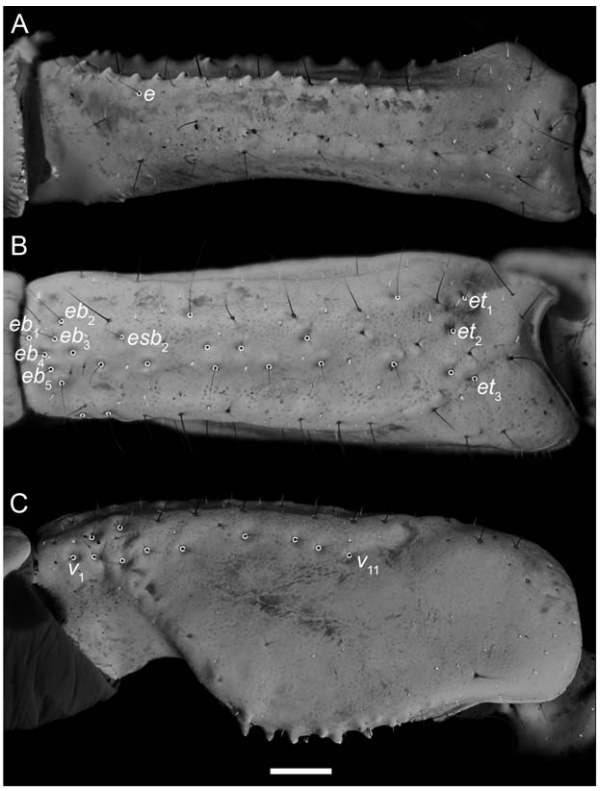

FIGURE 10. *Kolotl poncei* (Francke and Quijano-Ravell, 2009), n. comb., paratype ♂ (AMNH), dextral pedipalp femur, retrolateral aspect (**A**) and patella, retrolateral aspect (**B**) and ventral aspect (**C**), illustrating carinae and trichobothria. Scale bar = 1 mm. Abbreviations: ***e,*** external; ***eb,*** external basal; ***esb,*** external subbasal; ***et,*** external terminal; ***V,*** ventral.

Femur width greater than height; dorsal intercarinal surface flat, smooth, with few granules promedially; retrolateral intercarinal surface smooth (fig. 10A); ventral intercarinal surface flat, punctate; prolateral intercarinal surface coarsely and sparsely granular; dorsal prolateral carina well developed, comprising large spiniform granules; dorsal retrolateral carina moderately to weakly developed, comprising few large granules; ventral retrolateral carina obsolete; ventral prolateral carina moderately developed, comprising large spiniform granules.

Patella, dorsal, retrolateral and ventral intercarinal surfaces punctate; prolateral intercarinal surface finely and sparsely granular; proximal tubercle moderately developed, comprising two large granules; dorsal prolateral carina obsolete; dorsal median carina weakly to moderately developed, smooth; dorsal retrolateral, retrolateral median and ventral retrolateral carinae weakly developed to obsolete, smooth; ventral median carina obsolete; ventral prolateral carina moderately developed, comprising large spiniform granules.

Chela manus rounded, height greater than width; sparsely setose; dorsal intercarinal surface finely and sparsely granular to slightly reticulate; prolateral and retrolateral intercarinal surfaces punctate; dorsal median carina weakly developed, granular; dorsal secondary carina weakly developed, smooth; digital and ventral retrolateral carinae weakly developed

Downloaded From: https://bioone.org/journals/American-Museum-Novitates on 04 Jun 2024
Terms of Use: https://bioone.org/terms-of-use

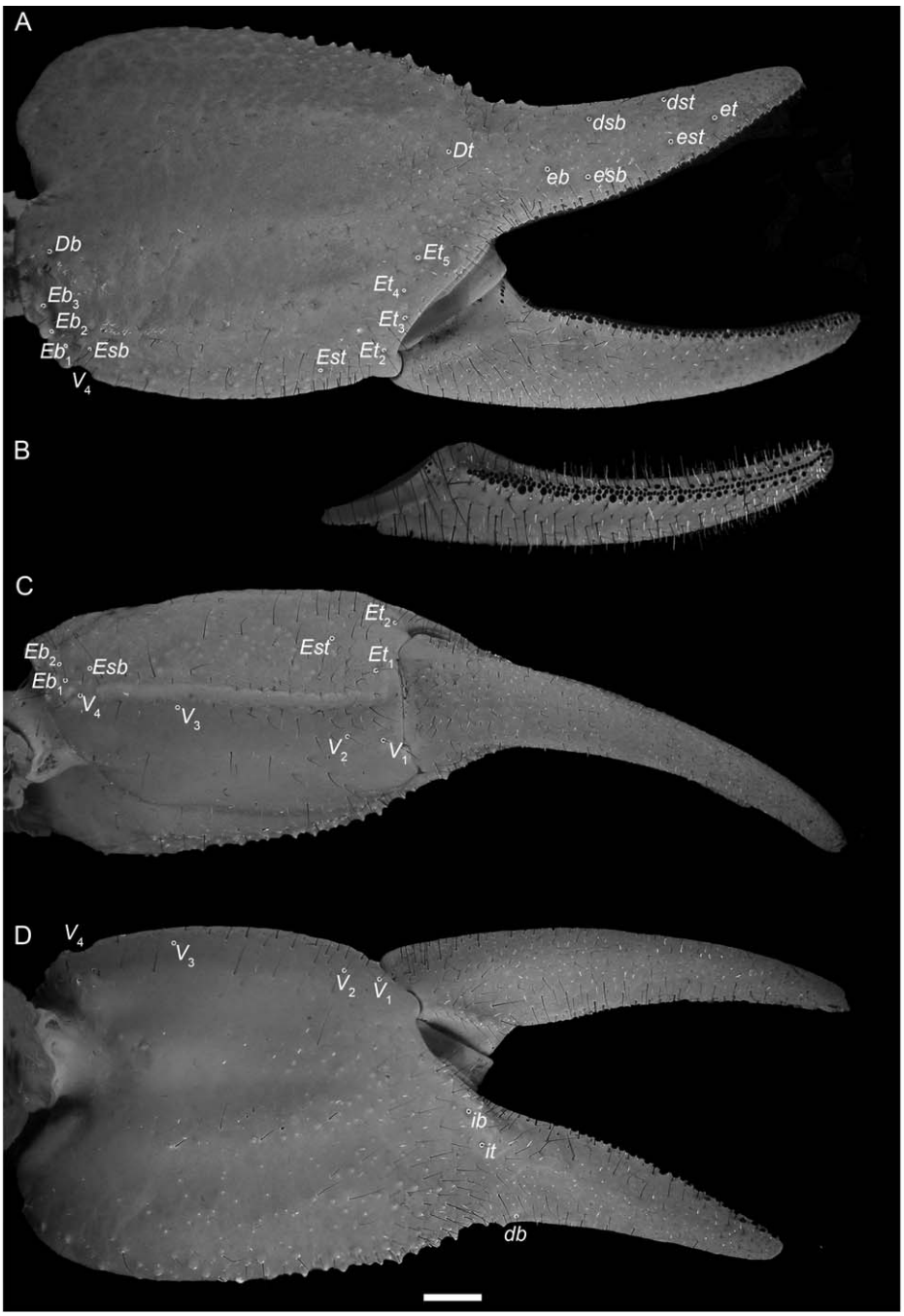

FIGURE 11. *Kolotl magnus* (Beutelspacher and López-Forment, 1991), n. comb., holotype ♀ (CNAN), dextral pedipalp chela, illustrating carinae and trichobothria. **A.** Retrodorsal aspect. **B.** Movable finger, dorsal aspect illustrating dentition. **C.** Ventral aspect. **D.** Proventral aspect. Scale bar = 1 mm. Abbreviations: ***Db*, *db*,** distal basal; ***dsb*,** distal subbasal; ***dst*,** distal subterminal; ***Dt*,** distal terminal; ***Eb*, *eb*,** external basal; ***Esb*, *esb*,** external subbasal; ***Est*, *est*,** external subterminal; ***Et*, *et*,** external terminal; ***ib*,** internal basal; ***it*,** internal terminal; ***V*,** ventral.

Downloaded From: https://bioone.org/journals/American-Museum-Novitates on 04 Jun 2024
Terms of Use: https://bioone.org/terms-of-use

to obsolete, smooth; retrolateral secondary carina weakly to moderately developed, smooth; dorsal secondary and retrolateral secondary carinae equally developed, more developed than digital carina; ventral median carina well developed, distal edge disconnected from retrolateral movable finger condyle and directed toward a point between prolateral and retrolateral movable finger condyles, less than half the distance between trichobothria Et_1 and V_1; ventral prolateral and prolateral ventral carinae obsolete; prolateral median and prolateral dorsal carinae weakly developed, granular. Chela fixed finger moderately curved; length less than femur length and patella length; dorsal surface punctate and moderately setose proximally; prolateral surface shallowly concave; retrolateral surface flat; prolateral carina weakly developed (fig. 12D, 13C). Chela movable finger, prolateral, median, and retrolateral denticle rows well defined from proximal quarter to tip of finger, and continuous, i.e., not interrupted by larger denticles (fig. 12B).

Legs: Legs I–IV, femora, and tibiae, prolateral surfaces shagreened. Basitarsi, spiniform macrosetae (fig. 14E–H), I: retrolateral distal, retrolateral subdistal, prolateral subdistal; II: prolateral distal, prolateral subdistal, retrolateral distal, retrolateral subdistal, retrolateral medial; III and IV: prolateral distal, ventral distal, ventral subdistal, retrolateral distal. Telotarsi, counts of spiniform macrosetae in pro- and retroventral rows, 3/5:4/6:5/7:5/7 (table 3).

Pectines: Tooth count: 16–19, mode = 17 (♂); 13–17, mode = 14 (♀) (table 2).

Mesosoma: Tergites I–VI, pretergites smooth, posttergites smooth to finely granular, VII, posterior margin finely granular. Sternites III–VII, smooth; VII, ventral submedian and ventral lateral carinae obsolete anteriorly, more strongly developed and smooth posteriorly.

Metasoma: Metasomal segments I–V, cross section terete; intercarinal surfaces smooth to finely granular, nongranular surfaces weakly punctate. Segments I–V, dorsal lateral carinae vestigial, comprising only one posterior granule on I, obsolete to weakly developed, granular on II, weakly to moderately developed, granular on III and IV; lateral supramedian carinae moderately to weakly developed, smooth to granular on I, granular to crenulate on II, weakly developed, granular on III and IV; lateral inframedian carinae weakly developed, smooth on I and II, weakly developed to obsolete on III and IV; ventral lateral carinae moderately developed, smooth to crenulate on I and II; weakly developed to obsolete, smooth on III and IV; ventral submedian carinae moderately developed, smooth on I and II; weakly developed to obsolete, smooth on III and IV. Segment V, dorsal lateral carinae moderately developed, granular to serrate; lateral inframedian carinae moderately developed, granular; ventral median carina strongly developed, comprising subspiniform granules; ventral transverse carina moderately developed, incomplete, comprising four (♂) or six (♀) large, subspiniform granules; anal arch semicircular, anal subterminal carina well developed, comprising 10 subspiniform granules, anal terminal carina moderately developed, granular.

Telson: Telson width/length ratio, 0.41 (♂), 0.45 (♀). Vesicle, dorsal surface smooth; lateral surfaces finely and sparsely granular to smooth; ventral surface coarsely granular anteriorly, smooth elsewhere. Subaculear tubercle stout, subconical.

Hemispermatophore: Lamelliform, weakly sclerotized; median lobe broad, margin with five crenulations (Francke and Quijano-Ravell, 2009).

Downloaded From: https://bioone.org/journals/American-Museum-Novitates on 04 Jun 2024
Terms of Use: https://bioone.org/terms-of-use

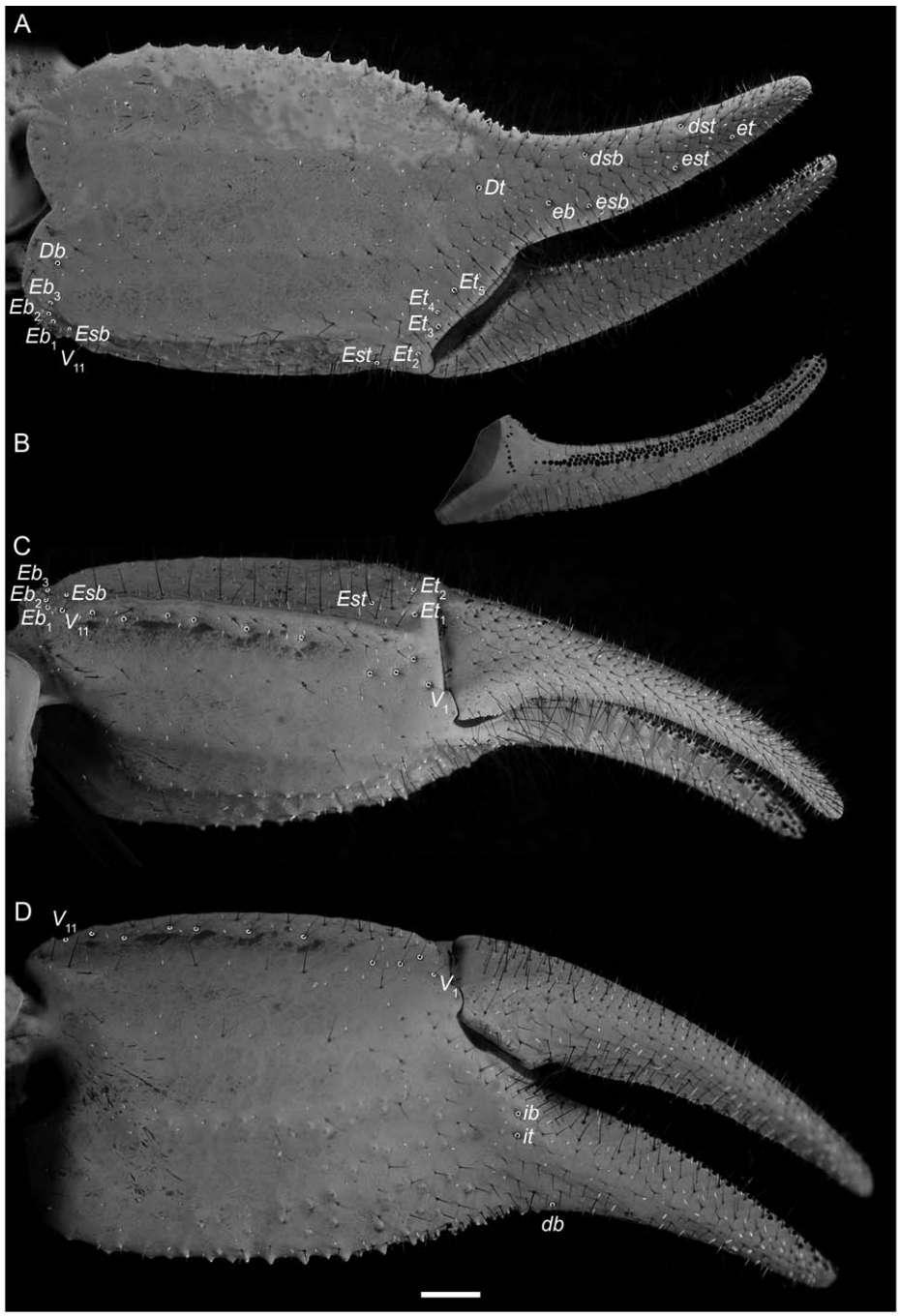

FIGURE 12. *Kolotl poncei* (Francke and Quijano-Ravell, 2009), paratype ♂ (AMNH), dextral pedipalp chela, illustrating carinae and trichobothria. **A.** Retrodorsal aspect. **B.** Movable finger, dorsal aspect illustrating dentition. **C.** Ventral aspect. **D.** Proventral aspect. Scale bar = 1 mm. Abbreviations: ***Db*, *db*,** distal basal; ***dsb*,** distal subbasal; ***dst*,** distal subterminal; ***Dt*,** distal terminal; ***Eb*, *eb*,** external basal; ***Esb*, *esb*,** external subbasal; ***Est*, *est*,** external subterminal; ***Et*, *et*,** external terminal; ***ib*,** internal basal; ***it*,** internal terminal; ***V*,** ventral.

Downloaded From: https://bioone.org/journals/American-Museum-Novitates on 04 Jun 2024
Terms of Use: https://bioone.org/terms-of-use

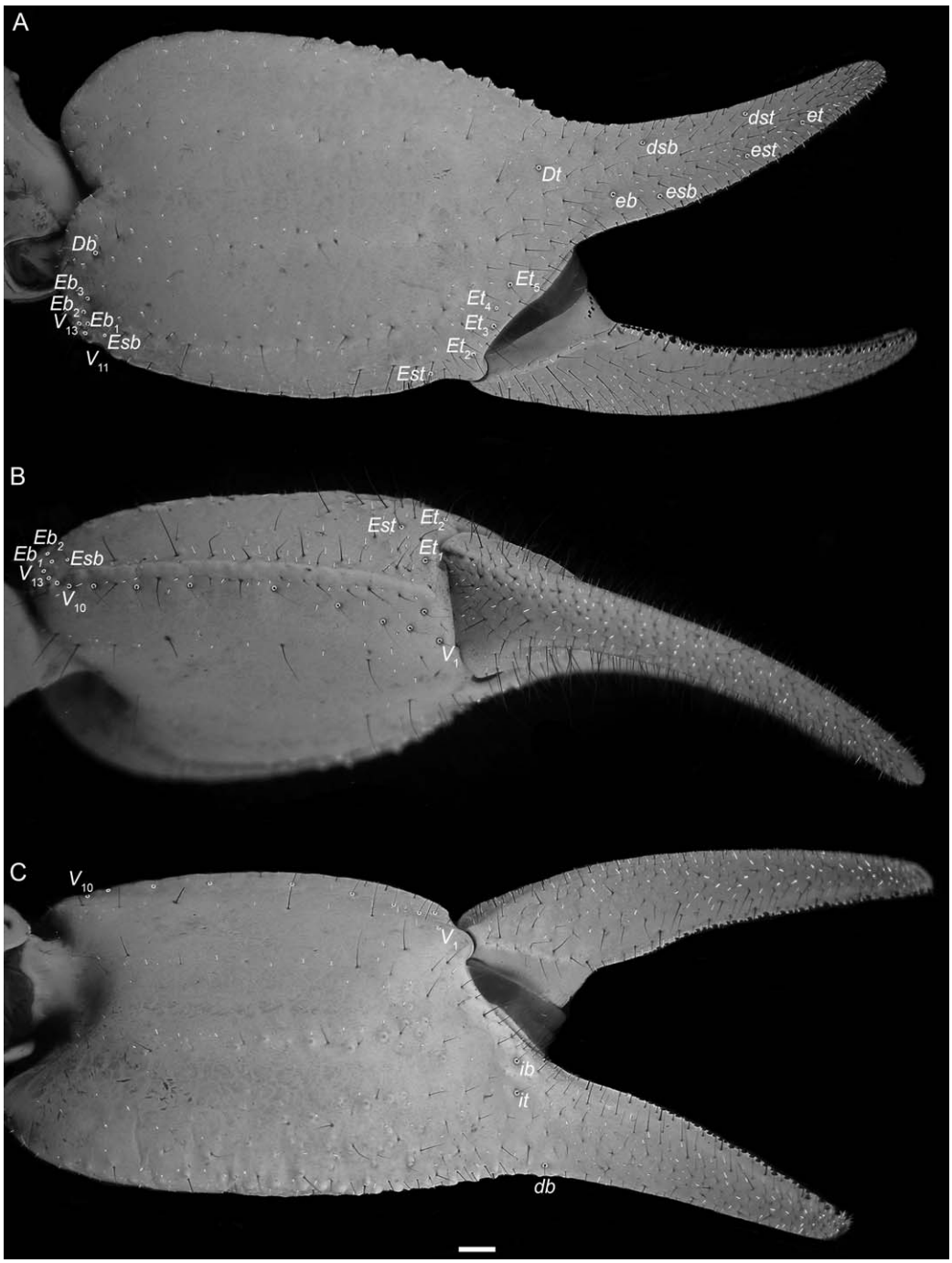

FIGURE 13. *Kolotl poncei* (Francke and Quijano-Ravell, 2009), paratype ♀ (CNAN), dextral pedipalp chela, illustrating carinae and trichobothria. **A.** Retrodorsal aspect. **B.** Ventral aspect. **C.** Proventral aspect. Scale bar = 1 mm. Abbreviations: ***Db*, *db*,** distal basal; ***dsb*,** distal subbasal; ***dst*,** distal subterminal; ***Dt*,** distal terminal; ***Eb*, *eb*,** external basal; ***Esb*, *esb*,** external subbasal; ***Est*, *est*,** external subterminal; ***Et*, *et*,** external terminal; ***ib*,** internal basal; ***it*,** internal terminal; ***V*,** ventral.

Downloaded From: https://bioone.org/journals/American-Museum-Novitates on 04 Jun 2024
Terms of Use: https://bioone.org/terms-of-use

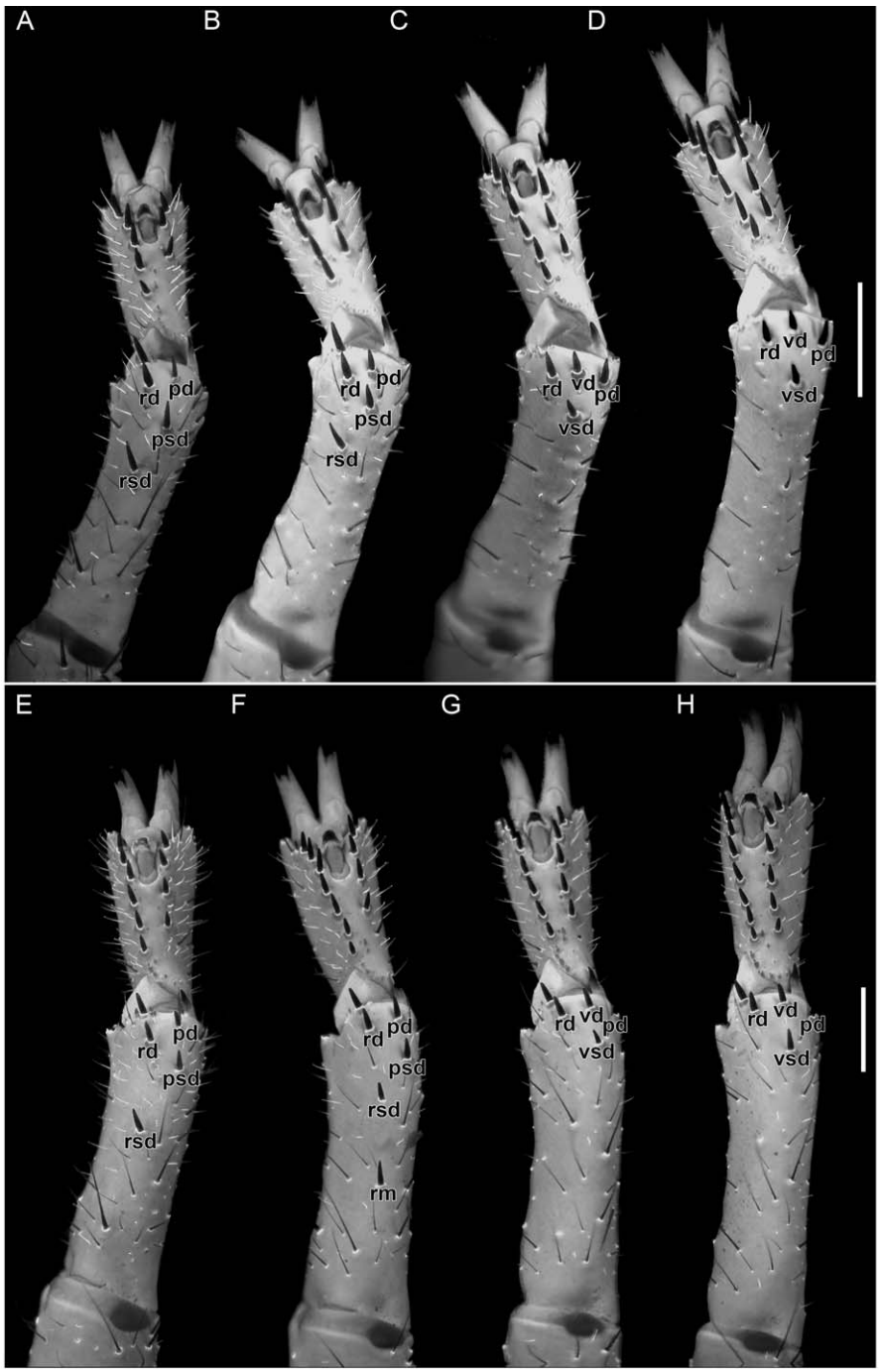

FIGURE 14. *Kolotl*, n. gen., legs I–IV, basitarsi and telotarsi, ventral aspect, illustrating pattern of spiniform macrosetae. **A–D.** *Kolotl magnus* (Beutelspacher and López-Forment, 1991), n. comb., holotype ♀ (CNAN). **E–H.** *Kolotl poncei* (Francke and Quijano-Ravell, 2009), n. comb., paratype ♂ (AMNH). Scale bars = 1 mm. Abbreviations: **pd,** prolateral distal; **psd,** prolateral subdistal; **rd,** retrolateral distal; **rm,** retrolateral medial; **rsd,** retrolateral subdistal; **vd,** ventral distal; **vsd,** ventral subdistal.

Downloaded From: https://bioone.org/journals/American-Museum-Novitates on 04 Jun 2024
Terms of Use: https://bioone.org/terms-of-use

Distribution: *Kolotl poncei* is known only from the type locality in the Municipio de La Huacana of southern Michoacan, Mexico (fig. 2).

Ecology: The species has been collected in rock crevices and under large, flat stones in tropical deciduous forest (fig. 3). The habitat and habitus are consistent with the semilithophilous ecomorphotype (Prendini, 2001).

ACKNOWLEDGMENTS

We thank A. Ballesteros, H. Montaño, J. Ponce, A. Quijano, and M. Villaseñor for assisting with fieldwork and/or providing material for study and analysis; J. Ponce for lending material from the CAFBUM collection; S. Thurston for assistance with preparing the plates for this contribution; and A. Contreras, J. Morrone, H. Ochoterena, J. Ponce, A. Zaldivar, and two anonymous reviewers for comments on previous drafts of the manuscript. Carlos E. Santibáñez-López was financially supported for his graduate studies by the Posgrado en Ciencias Biologicas of UNAM and Consejo Nacional de Ciencias y Tecnologia (CONACYT), and received a Collections Study Grant (2011) and a Theodore Roosevelt Memorial Grant (2012) from the AMNH to support his visits to New York. Fieldwork in Mexico was conducted under scientific permit FAUT-0175 from Secretaría del Medio Ambiente y Recursos Naturales (SEMARNAT), and partially supported by a grant from the Instituto Bioclon to Oscar F. Francke, and by U.S. National Science Foundation grant DEB 0413453 to Lorenzo Prendini.

REFERENCES

Beutelspacher, C.R. 2000. Catálogo de los alacranes de México. Morelia, Michoacán: Universidad Michoacana de San Nicolás de Hidalgo, 175 pp.

Beutelspacher, C.R., and C.W. López Forment. 1991. Una nueva especie de *Diplocentrus* (Scorpionida: Diplocentridae) en México. Anales del Instituto de Biología, Universidad Nacional Autónoma de México, Serie Zoológica 62 (1): 33–40.

Contreras-Félix, G., and C.E. Santibáñez-López. 2011. *Diplocentrus bicolor* sp. n. (Scorpiones: Diplocentridae) from Jalisco, Mexico. Zootaxa 2992: 61–68

Francke, O.F. 1977. Scorpions of the genus *Diplocentrus* from Oaxaca, Mexico (Scorpionida, Diplocentridae). Journal of Arachnology 4: 145–200.

Francke, O.F. 1978. Systematic revision of diplocentrid scorpions from circum-Caribbean lands. Special Publications of the Museum, Texas Tech University 14: 1–92.

Francke, O.F., and A. Quijano-Ravell. 2009. Una especie nueva de *Diplocentrus* (Scorpiones: Diplocentridae) del estado de Michoacán, México. Revista Mexicana de Biodiversidad 80: 659–663.

Fritts, D.A., and W.D. Sissom. 1996. Two new *Diplocentrus* (Scorpiones, Diplocentridae) from Mexico. Entomological News 107: 39–48.

Hadley, A. 2008. CombineZM. Online resource (http://hadleyweb.pwp.blueyonder.co.uk/), accessed September 2011.

Jarvis A., H.I. Reuter, A. Nelson, and E. Guevara. 2008. Hole-filled seamless SRTM data Ver. 4. International Centre for Tropical Agriculture. Online resource (http://srtm.csi.cgiar.org), accessed September, 2012.

Downloaded From: https://bioone.org/journals/American-Museum-Novitates on 04 Jun 2024
Terms of Use: https://bioone.org/terms-of-use

Kovařík, F. 1998. Štiři (Scorpions). Jihlava, Czech Republic: Madagaskar. 175 pp. [in Czech]

Mattoni, C., J.A. Ochoa, A.A. Ojanguren-Affilastro and L. Prendini. 2012. *Orobothriurus* (Scorpiones: Bothriuridae) phylogeny, Andean biogeography, and the relative importance of genitalic and somatic characters. Zoologica Scripta 41: 160–176.

Prendini, L. 2000. Phylogeny and classification of the superfamily Scorpionoidea Latreille 1802 (Chelicerata, Scorpiones): an exemplar approach. Cladistics 16: 1–78.

Prendini, L. 2001. Substratum specialization and speciation in southern African scorpions: the Effect Hypothesis revisited. *In* V. Fet and P.A Selden (editors), Scorpions 2001. In memoriam Gary A. Polis: 113–118. Burnham Beeches, UK: British Arachnological Society.

Prendini, L., and W.C. Wheeler. 2005. Scorpion higher phylogeny and classification, taxonomic anarchy, and standards for peer review in online publishing. Cladistics 21: 446–494.

Prendini, L., T.M. Crowe, and W.C. Wheeler. 2003. Systematics and biogeography of the family Scorpionidae (Chelicerata: Scorpiones), with a discussion on phylogenetic methods. Invertebrate Systematics 17: 185–259.

Santibáñez-López, C.E., O.F. Francke, and L. Prendini. 2013a. Systematics of the *keyserlingii* group of *Diplocentrus* Peters, 1861 (Scorpiones: Diplocentridae), with descriptions of three new species from Oaxaca, Mexico. American Museum Novitates 3777: 1–47.

Santibáñez-López, C.E., O.F. Francke, and A. Ortega-Gutierrez. 2013b. Variation in the spiniform macrosetae pattern on the basitarsi of *Diplocentrus tehuacanus* (Scorpiones: Diplocentridae): new characters to diagnose species within the genus. Journal of Arachnology 41: 319–326.

Santibáñez-López, C.E., O.F. Francke, and L. Prendini. In press. Phylogeny of the North American scorpion genus *Diplocentrus* Peters, 1861 (Scorpiones: Diplocentridae) based on morphology, nuclear and mitochondrial DNA. Arthropod Systematics and Phylogeny.

Sissom, W.D. 1990. Systematics, biogeography and paleontology. *In* G.A. Polis (editor), The biology of scorpions: 64–160. Stanford, CA: Stanford University Press.

Sissom, W.D., and V. Fet. 2000. Family Diplocentridae Karsch, 1880. *In* V. Fet, W.D. Sissom, G. Lowe, and M.E. Braunwalder, Catalog of the scorpions of the world (1758–1998): 329–354. New York: New York Entomological Society.

Sissom, W.D., and J.R. Reddell. 2009. Cave scorpions of Mexico and the United States. Studies on the cave and endogean fauna of North America V. Texas Memorial Museum, Speleological Monographs 7: 19–32.

Soleglad, M.E., and W.D. Sissom. 2001. Phylogeny of the family Euscorpiidae Laurie, 1896: a major revision. *In* V. Fet and P.A. Selden (editors), Scorpions 2001. In memoriam Gary A. Polis: 25–111. Burnham Beeches, UK: British Arachnological Society.

Stahnke, H.L. 1970. Scorpion nomenclature and mensuration. Entomological News 81: 297–316.

Stockwell, S.A. 1992. Systematic observations on North American Scorpionida with a key and checklist of the families and genera. Journal of Medical Entomology 29: 407–422.

Teruel, R. 2003. Un nuevo escorpión del género *Diplocentrus* Peters, 1861 (Scorpiones: Diplocentridae) del estado de Guerrero, México. Revista Ibérica de Aracnología 76: 49–53.

Vachon, M. 1973 [1974]. Étude des caractères utilisés pour classer les familles et les genres de scorpions (Arachnides). 1. La trichobothriotaxie en arachnologie. Sigles trichobothriaux et types de trichobothriotaxie chez les scorpions. Bulletin du Muséum National d'Histoire Naturelle 3: 857–958.

Volschenk, E.S., and L. Prendini. 2008. *Aops oncodactylys*, gen. et sp. nov., the first troglobitic urodacid (Urodacidae: Scorpiones), with a re-assessment of cavernicolous, troglobitic and troglomorphic scorpions. Invertebrate Systematics 22: 235–257.

Williams, S.C., and V.F. Lee. 1975. Diplocentrid scorpions from Baja California Sur, Mexico (Scorpionida: Diplocentridae). Occasional Papers of the California Academy of Sciences 115: 1–27.

Downloaded From: https://bioone.org/journals/American-Museum-Novitates on 04 Jun 2024
Terms of Use: https://bioone.org/terms-of-use

APPENDIX 1

List of 95 Morphological Characters Scored for Cladistic Analysis of 35 Species in Six Diplocentrid Scorpion Genera (Santibáñez-López et al., in press).

Characters from previous analyses that correspond partially or entirely to those in the present list are indicated in brackets by the following abbreviations P00 (Prendini 2000), PEA03 (Prendini et al., 2003) and MEA12 (Mattoni et al., 2012), followed by the character number from the corresponding publication. Fifteen uninformative characters (excluded from all analyses) are indicated by †.

Pigmentation Pattern

0. Base coloration: dark brown to black (0); reddish (1); orange-brown (2); yellowish (3).
1. Chelicerae, infuscation: absent (0); present (1) [PEA03:90].
2. Metasoma dorsal and lateral carinae, coloration relative to adjacent intercarinal surfaces: darker (0); similar (1).
3. Pedipalp chela manus, dorsal secondary carina, coloration relative to adjacent intercarinal surfaces (♂): darker (0); similar (1).
4. Pedipalp chela manus, digital carina, coloration relative to adjacent intercarinal surfaces (♂): darker (0); similar (1).
5. Pedipalp chela manus, retrolateral secondary carina, coloration relative to adjacent intercarinal surfaces (♂): darker (0); similar (1).
6. Pedipalp chela fingertips, coloration relative to chela manus: similar (0); darker (1); paler (2).
7. Pedipalp chela manus, dorsal secondary carina, coloration relative to adjacent intercarinal surfaces (♀): darker (0); similar (1).
8. Pedipalp chela manus, digital carina, coloration relative to adjacent intercarinal surfaces (♀): darker (0); similar (1).
9. Pedipalp chela manus, retrolateral secondary carina, coloration relative to adjacent intercarinal surfaces (♀): darker (0); similar (1).
10. Legs, coloration relative to mesosomal tergites: similar (0); paler (1).
11. Legs, infuscation: absent (0); present (1) [PEA03:99].

Chelicerae

12. Movable finger subdistal tooth, length relative to medial tooth: smaller (0); similar (1).
13. Movable finger ventral distal tooth, length relative to dorsal distal tooth: equal (0); subequal, i.e., greater than half (1); unequal, i.e., less than half (2) [PEA03:2].

Carapace

14. Median ocular tubercle, protrusion: raised (0); level (1). [P00:2].
15. Median longitudinal sulcus, width: narrow (0); broad (1) [P00:4].
16. Anteromedian longitudinal sulcus, length: complete (0); vestigial (1) [MEA12:7].

†17. Lateral ocelli, number of pairs: 3 (0); 2 (1); 0 (2) [P00:1].

18. Nongranular surfaces, punctation: absent (0); present (1).

Pedipalp Carination and Surface Macrosculpture

19. Pedipalp femur intercarinal surfaces: uniformly granular (0); granular medially (1); smooth (2).
20. Pedipalp femur nongranular intercarinal surfaces, punctation: present (0); absent (1).
21. Femur dorsal intercarinal surface, shape: flat (0); shallowly convex (1); markedly convex (2) [PEA03:40; MEA12:10].

Downloaded From: https://bioone.org/journals/American-Museum-Novitates on 04 Jun 2024
Terms of Use: https://bioone.org/terms-of-use

22. Patella dorsal retrolateral carina, development (♂): distinct, i.e., raised above adjacent intercarinal surfaces (0); obsolete, i.e., not raised above adjacent intercarinal surfaces (evident as difference in texture or pigmentation) (1) [PEA03:42].
23. Patella dorsal retrolateral carina, texture (♂): granular (0); smooth (1).
24. Patella dorsal retrolateral carina, development (♀): distinct (0); obsolete (1) [P00:17]
†25. Patella dorsal retrolateral carina, texture (♀): granular (0); smooth (1).
26. Patella retrolateral median carina, development (♂): distinct (0); obsolete (1).
27. Patella retrolateral median carina, texture (♂): granular (0); smooth (1).
28. Patella retrolateral median carina, development (♀): distinct (0); obsolete (1).
†29. Patella retrolateral median carina, texture (♀): granular (0); smooth (1).
30. Patella ventral median carina (♂): absent (0); granular (1); smooth (2).
31. Chela manus, dorsal secondary carina, development (♂): distinct (0); obsolete (1) [P00:20; PEA03:31].
32. Chela manus, dorsal secondary carina, texture (♂): smooth (0); granular to crenulate (1).
33. Chela manus, dorsal secondary carina, development (♀): distinct (0); obsolete (1) [P00:21].
34. Chela manus, dorsal secondary carina, texture (♀): smooth (0); granular to crenulate (1).
35. Chela manus, digital carina, development (♂): distinct (0); obsolete (1) [P00:23; PEA03:32].
36. Chela manus, digital carina, texture (♂): smooth (0); granular (1).
37. Chela manus, digital carina, length (♂): base of manus to tip of fixed finger (0); base of manus to base of fixed finger (1) [PEA03:32].
38. Chela manus, digital carina, development (♀): distinct (0); obsolete (1) [P00:23].
39. Chela manus, digital carina, texture (♀): smooth (0); granular (1).
40. Chela manus, digital carina, length (♀): base of manus to tip of fixed finger (0); base of manus to base of fixed finger (1).
41. Chela manus, dorsal secondary, digital and retrolateral secondary carinae, relative development (♂): digital carina more developed than dorsal secondary and retrolateral secondary carinae (0); dorsal secondary, digital, and retrolateral secondary carinae similarly developed (1); dorsal secondary and retrolateral secondary carinae more developed than digital carina (2) [P00:24].
42. Chela manus, dorsal secondary, digital, and retrolateral secondary carinae, relative development (♀): digital carina more developed than dorsal secondary and retrolateral secondary carinae (0); dorsal secondary, digital, and retrolateral secondary carinae similarly developed (1); dorsal secondary and retrolateral secondary carinae more developed than digital carina (2) [P00:24].
43. Chela manus, retrolateral secondary carina, texture (♂): smooth (0); granular (1).
44. Chela manus, retrolateral secondary carina, texture (♀): smooth (0); granular to crenulate (1).
45. Chela manus, dorsal margin, curvature relative to digital carina (♂): convex, not parallel to digital carina (0); subparallel to digital carina (1); parallel to digital carina (2) [MEA12:15].
46. Chela manus, dorsal margin, curvature relative to digital carina (♀): convex, not parallel to digital carina (0); subparallel to digital carina (1).
47. Chela manus, ventral median carina, orientation of distal edge relative to trichobothria Et_1 and V_1: directed toward Et_1 (0); directed toward a point less than half the distance between Et_1 and V_1 (1); directed toward a point approximately half the distance between Et_1 and V_1 (2); directed toward a point more than half the distance between Et_1 and V_1 (3); directed toward V_1 (4). [P00:27]
†48. Chela manus, dorsal marginal carina length: base of manus to base of fixed finger (0); base of manus to tip of fixed finger (1).
49. Chela manus, intercarinal surfaces (♂): smooth (0); granular (1); reticulate (2) [MEA12:29].
50. Chela manus, intercarinal surfaces (♀): smooth (0); granular (1); reticulate (2) [MEA12:30].
51. Chela manus, nongranular intercarinal surfaces, punctation: present (0); absent (1).

Downloaded From: https://bioone.org/journals/American-Museum-Novitates on 04 Jun 2024
Terms of Use: https://bioone.org/terms-of-use

52. Chela fixed finger, prolateral concavity, proximal to *ib* and *it* trichobothria (♂): weakly developed, shallow (0); well developed, deep (1).

Pedipalp Chela Finger Dentition

53. Chela movable finger, median denticle row, development: distinct from base to tip of finger (0); weakly defined in basal third of finger, indistinct from prolateral denticle row (1).
54. Chela movable finger, median denticle row: discontinuous, interrupted by larger denticles (0); continuous, not interrupted by larger denticles (1).
†55. Chela movable finger, median denticle row, first and second denticles, size relative to other denticles: larger (0); similar (1).
56. Chela movable finger, retrolateral denticle row, disposition: parallel to median denticle row from second large median denticle to tip of finger (0); parallel to median denticle row from base to tip of finger (1).
57. Chela movable finger, prolateral denticle row, disposition: parallel to median denticle row from second large median denticle to tip of finger (0); parallel to median denticle row from base to tip of finger (1).

Pedipalp Trichobothria

†58. Patella, ventral surface, *v* trichobothria, number: 3 (0); 4, i.e., one accessory (1); 12–18, i.e., 8–14 accessories (2).
†59. Patella, retrolateral surface, *et* trichobothria, number: 3 (0); 4 (1).
†60. Patella, retrolateral surface, *est* trichobothria, number: 2 (0); 3 (1).
†61. Patella, retrolateral surface, *em* trichobothria, number: 2 (0); 3 (1); 4 (2).
†62. Patella, retrolateral surface, *esb* trichobothria, number: 2 (0); 5 (1).
†63. Patella, retrolateral surface, *eb* trichobothria, number: 5 (0); 6 (1).
64. Chela manus (♂), trichobothrium *ib*, position relative to articulation between fixed and movable fingers: aligned (0); distal (1).
65. Chela manus (♂), trichobothrium *it*, position relative to trichobothrium *ib*: aligned (0); distal (1).
†66. Chela manus, ventral surface, *V* trichobothria, number: 4 (0); more than 4, i.e., 5–9 accessories (1).

Legs

67. Leg telotarsi, laterodistal lobes: truncate (0); rounded (1) [P00:65].
68. Leg lateral surfaces, punctation: absent (0); present (1).
†69. Leg basitarsi, prolateral pores (♂): absent (0); present (1) [P00:67].
70. Leg I basitarsus, proventral distal spiniform macroseta: absent (0); present (1).
71. Leg I basitarsus, retroventral distal spiniform macroseta: absent (0); present (1).
72. Leg I basitarsus, proventral subdistal spiniform macroseta: absent (0); present (1).
73. Leg I basitarsus, retroventral subdistal spiniform macroseta: absent (0); present (1).
74. Leg I basitarsus, proventral medial spiniform macroseta: absent (0); present (1).
75. Leg I basitarsus, retroventral medial spiniform macroseta: absent (0); present (1).
76. Leg I basitarsus, retrolateral medial spiniform macroseta: absent (0); present (1).
77. Leg II basitarsus, proventral distal spiniform macroseta: absent (0); present (1).
†78. Leg II basitarsus, retroventral distal spiniform macroseta: absent (0); present (1).
79. Leg II basitarsus, proventral subdistal spiniform macroseta: absent (0); present (1).
80. Leg II basitarsus, retroventral subdistal spiniform macroseta: absent (0); present (1).
81. Leg II basitarsus, proventral medial spiniform macroseta: absent (0); present (1).

Downloaded From: https://bioone.org/journals/American-Museum-Novitates on 04 Jun 2024
Terms of Use: https://bioone.org/terms-of-use

82. Leg II basitarsus, retroventral medial spiniform macroseta: absent (0); present (1).
83. Leg II basitarsus, retroventral submedial spiniform macroseta: absent (0); present (1).
84. Leg II basitarsus, ventral distal spiniform macroseta: absent (0); present (1).
85. Leg II basitarsus, retroventral subbasal spiniform macroseta: absent (0); present (1).
†86. Leg II basitarsus, retrolateral subdistal spiniform macroseta: absent (0); present (1).
87. Leg II basitarsus, retrolateral medial spiniform macroseta: absent (0); present (1).
88. Leg II basitarsus, retrolateral subbasal macroseta: absent (0); present, spiniform (1); present, setiform (2).
89. Legs III and IV basitarsi, retroventral subdistal spiniform macrosetae: absent (0); present (1).
90. Legs III and IV basitarsi, ventral medial spiniform macrosetae: absent (0); present (1).

Mesosoma, Metasoma and Telson

91. Sternite VII median carina, development: distinct (0); obsolete (1).
92. Sternite VII median carina, length relative to submedian carinae: equal to (0); less than (1).
93. Sternite VII submedian carinae, development: distinct (0); obsolete (1) [PEA03:102, 103].
94. Mesosoma, metasoma and telson, nongranular dorsal surfaces, punctation: absent (0); present (1).

All issues of *Novitates* and *Bulletin* are available on the web (http://digitallibrary.amnh.org/dspace). Order printed copies on the web from:
http://shop.amnh.org/a701/shop-by-category/books/scientific-publications.html

or via standard mail from:
American Museum of Natural History—Scientific Publications
Central Park West at 79th Street
New York, NY 10024

♾ This paper meets the requirements of ANSI/NISO Z39.48-1992 (permanence of paper).

Downloaded From: https://bioone.org/journals/American-Museum-Novitates on 04 Jun 2024
Terms of Use: https://bioone.org/terms-of-use